Int. J. Solids Structures Vol. 16, pp. 71–95

0020-7683/80/0101-0001/$02.00/0

LARGE DISPLACEMENT THEORY OF THIN-WALLED CURVED MEMBERS AND ITS APPLICATION TO LATERAL-TORSIONAL BUCKLING ANALYSIS OF CIRCULAR ARCHES

T. USAMI† and S. Y. KOH

Division of Structural Engineering and Construction, Asian Institute of Technology, P.O. Box 2754, Bangkok, Thailand

(*Received* 12 *June* 1978; *in revised form* 26 *March* 1979)

Abstract—The purpose of this study is to establish a one dimensional large displacement theory for plane-curved members with thin-walled open sections. Consequently, this theory is applied in the analysis of lateral-torsional buckling of circular arches. Typical numerical examples are shown herein to illustrate how the ratio of different types of rigidities in non-dimensional form affects the buckling loads.

NOTATION

A area of cross section
a rise of a circular arch (Fig. 3)
b span of a circular arch (Fig. 3)
$d^{(0)}$ $= u_s^{(0)\prime} - w_s^{(0)}$
E modulus of elasticity
f quantity defined in eqn (20a)
G shear modulus
g quantity defined in eqn (20b)
h_c distance between the applied uniformly distributed loads on the horizontal projection and the crown of circular arch (Fig. 3)
I_x, I_y, I_{xy} moments of inertia about x, y axes and product of inertia
I_ω warping moment of inertia
$I_{\omega x}, I_{\omega y}, I_{\omega xy}$ warping product of inertia about x and y axes defined by eqns (30) and (52)
$K_x, K_y, K_{xy}, K_\omega, K_{\omega x}, K_{\omega y}$ stress resultants defined in eqns (28)
K_T St. Venant torsional constant
L arc length of a circular arch
l, m direction cosines defined by eqns (7)
M_x, M_y, M_ω, N bending moments about x, y axes, bimoment, axial force
$\bar{M}_x, \bar{M}_y, \bar{M}_\omega, \bar{N}$ stress resultants defined in eqns (28)
n, s, θ curvilinear coordinate system (Fig. 2)
$\bar{q}_x, \bar{q}_y, \bar{q}_\theta$ externally applied uniformly distributed loads defined in eqns (27)
q uniformly distributed load applied on the horizontal projection
R_c, R_0, R_s radii of curvature of points C, O, S
r radius of curvature of an arbitrary point on the cross section
u, v, w displacement components in x, y, θ directions
u_s, v_s, w_s displacement components of point S in x, y, θ directions
u_p, w_p displacement components in x, θ directions at the point of applying the external forces
w_c displacement components of point C in θ direction
x, y, θ cylindrical coordinate system with origin at point O (Fig. 2)
x_c, y_c x and y coordinate of point C
x_s, y_s x and y coordinate of point S
$\alpha, \gamma, \kappa, \bar{\kappa}, \psi, \mu$ non-dimensional parameters defined by eqns (51) and eqn (42h)
δ variational operator
Γ, Φ_1, Φ_2 quantities defined by eqns (42)
$\epsilon_x, \epsilon_y, \epsilon_\theta, \gamma_{xy}, \gamma_{y\theta}, \gamma_{x\theta}$ strain components in x, y, θ coordinate system
$\gamma_{\theta n}, \gamma_{\theta s}$ shear strains components on θs and θn planes
β angle of twist
λ non-dimensional form of buckling load defined by eqn (50)
ρ_n, ρ_s normal and tangtential distance in n, s directions defined by eqns (7)
ξ, η displacement components of any point on the cross section in the n and s directions
$\phi_{\beta i}, \phi_{vi}$ displacement functions
ω unit warping defined by eqn (20c)

†Present address: Department of Civil Engineering, Faculty of Engineering, Gifu University, Gifu, Japan.

Ω^*, Ω_r^* quantities defined by eqns (18)
θ_1, θ_2 values of θ at both ends of the curved member
θ_0 half of the subtended angle of circular arch
$(\ )^*$ denotes the quantity defined along the middle line of thin wall
$(\ )'$ $(\mathrm{d}/\mathrm{d}\theta)(\ )$
$(\ )^{(0)}$ denotes the quantity at initial stage before buckling

1. INTRODUCTION

A structural member is called thin-walled member if its thickness is relatively small as compared with any characteristic dimension of its cross section, and the cross-sectional dimensions are small as compared with its length. Due to the small thickness, thin-walled members possessing maximum stiffnesses for minimum weight are extensively used in engineering practices. They may be the roofs of industrial buildings on earth, the long span main girders of a bridge across a river, the wings and fuselages of an airplane in the air, the hull of a ship on the sea or a submarine in the sea, as well as of a rocket in space.

The linear elastic behavior of thin-walled curved members under various types of loading has been studied by numerous investigators[1–11]. Nishino and Fukasawa[11] have classified those studies into three categories depending on the accuracy of treating the geometry of curved members. In the first approach, the initial radius of curvature of the member is assumed to be large so that its difference over the cross section is entirely ignored. Vlasov's work[1] belongs to this category. In the studies of the second category, although the difference between the initial radius of curvature of the centroid and the shear center of the cross section is considered in the formulations, the cross-sectional properties obtained are the same as those for straight members. The works by Cheney[4] and by Dabrowski[7, 8] belong to this category. In the third approach, which is considered to be the most rigorous analysis, the difference of initial radius of curvature of the member over the cross section is taken into consideration and the cross-sectional properties are defined as functions of an initial radius of curvature of an arbitrary point on the cross section. Konishi and Komatsu[2, 3], Kuranishi[5], Fukasawa[6], Nitzsche and Miller[9], Williams[10], and Nishino and Fukasawa[11] have developed their theories using this approach.

Although linear elastic analysis of thin-walled curved members are well established, only a few studies have been published on large displacement theory of thin-walled curved members. Namita[12] derived equations of equilibrium from geometric considerations of the deformed curved members and applied them to the analysis of lateral-torsional buckling of circular arches. Namita's theory belongs to the first category in the above classification. Enda[13, 14] analyzed large displacement behavior of horizontally curved girders. He derived the fundamental equations of equilibrium from geometric considerations of the deformed plane-curved members[13] as well as from the principle of minimum potential energy for initial stress problems[14, 15]. His theory also belongs to the first category. A more rigorous nonlinear theory of curved beams has been developed by Usuki[16], who integrated the Novozhilov's nonlinear strain-displacement equations for thin shells of revolution[17] to obtain the relations between strain and displacement components of an arbitrary point on the cross section of a curved member. The theory has been applied to the analysis of lateral-torsional buckling of circular arches subjected to equal end moments. More recently, Nair and Hegemier[18] succeeded in deriving a system of linear equations governing the small deformations of an initially stressed, curved member through the use of the principle of virtual work for initial stress problems[15]. Transverse shear deformations are particularly incorporated into the formulations, but the warping torsional effects are not considered.

In this study, a rigorous large displacement theory of curved members, which belongs to the third category, is presented. The approach of this study is basically the extension of the large displacement theory of thin-walled straight members developed by Nishino *et al.*[19, 20] to the thin-walled curved members with open sections. This large displacement theory will be established from a set of simple and realistic assumptions, which have normally been used in thin-walled beams analysis, and the variational principles in elasticity. The advantage of this approach is that the geometry of the deformed curved members need not be considered in the formulations.

The merit of this established large displacement theory will be further illustrated by its application in the analysis of lateral-torsional buckling of circular arches. The governing equation for lateral-torsional buckling is derived by using the derived strain-displacement relations through the Euler method in a variational principle. A typical example will be shown to illustrate how the different values of non-dimensional parameters, in term of the ratio of different types of rigidities, affect the buckling loads of circular arches with thin-walled open sections.

2. VARIATIONAL FORMULATION FOR CURVED MEMBERS WITH THIN-WALLED OPEN SECTIONS

2.1 *Basic assumptions*

In this study, a set of basic assumptions which have normally been made in the thin-walled beams analysis, are used in the formulations. The pertinent assumptions in this regard are as follows: (1) the length of the member is much larger than any cross section dimensions; (2) the displacements are small but finite; (3) the cross sections do not distort; (4) the shear strains due to shear stress in equilibrium with the changes of normal stresses are small and can be neglected (Euler–Bernouli hypothesis); (5) the shear strains in the planes normal to the middle surface of thin walls are small and can be neglected.

2.2 *Three-dimensional strain-displacement relations in cylindrical coordinate system*

Consider a circular curved member with the center of curvature O' as shown in Fig. 1. The general three dimensional finite strain-displacement relations, in cylindrical coordinate system

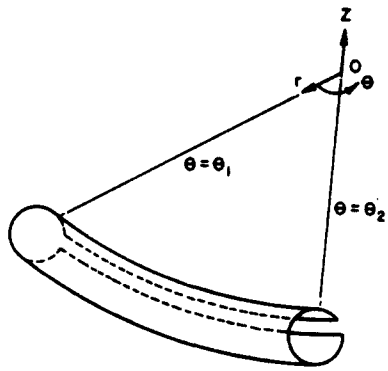

Fig. 1. Curved member with thin-walled section.

(r, θ, z), which could be derived from tensor calculus and differential geometry, as indicated by Washizu[15], are given in the following:

$$\epsilon_r = \frac{\partial u_r}{\partial r} + \frac{1}{2}\left[\left(\frac{\partial u_r}{\partial r}\right)^2 + \left(\frac{\partial u_\theta}{\partial r}\right)^2 + \left(\frac{\partial u_z}{\partial r}\right)^2\right] \tag{1a}$$

$$\epsilon_\theta = \frac{1}{r}\frac{\partial u_\theta}{\partial \theta} + \frac{u_r}{r} + \frac{1}{2r^2}\left[\left(\frac{\partial u_r}{\partial \theta} - u_\theta\right)^2 + \left(\frac{\partial u_\theta}{\partial \theta} + u_r\right)^2 + \left(\frac{\partial u_z}{\partial \theta}\right)^2\right] \tag{1b}$$

$$\epsilon_z = \frac{\partial u_z}{\partial z} + \frac{1}{2}\left[\left(\frac{\partial u_r}{\partial z}\right)^2 + \left(\frac{\partial u_\theta}{\partial z}\right)^2 + \left(\frac{\partial u_z}{\partial z}\right)^2\right] \tag{1c}$$

$$\gamma_{r\theta} = \frac{1}{r}\frac{\partial u_r}{\partial \theta} - \frac{u_\theta}{r} + \frac{\partial u_\theta}{\partial r} + \frac{1}{r}\frac{\partial u_r}{\partial r}\frac{\partial u_r}{\partial \theta} - \frac{u_\theta}{r}\frac{\partial u_r}{\partial r} + \frac{1}{r}\frac{\partial u_\theta}{\partial r}\frac{\partial u_\theta}{\partial \theta} + \frac{u_r}{r}\frac{\partial u_\theta}{\partial r} + \frac{1}{r}\frac{\partial u_z}{\partial r}\frac{\partial u_z}{\partial \theta} \tag{1d}$$

$$\gamma_{\theta z} = \frac{\partial u_\theta}{\partial z} + \frac{1}{r}\frac{\partial u_z}{\partial \theta} + \frac{1}{r}\frac{\partial u_r}{\partial z}\frac{\partial u_r}{\partial \theta} - \frac{u_\theta}{r}\frac{\partial u_r}{\partial z} + \frac{1}{r}\frac{\partial u_\theta}{\partial \theta}\frac{\partial u_\theta}{\partial z} + \frac{u_r}{r}\frac{\partial u_\theta}{\partial z} + \frac{1}{r}\frac{\partial u_z}{\partial \theta}\frac{\partial u_z}{\partial z} \tag{1e}$$

$$\gamma_{zr} = \frac{\partial u_r}{\partial z} + \frac{\partial u_z}{\partial r} + \frac{\partial u_r}{\partial r}\frac{\partial u_r}{\partial z} + \frac{\partial u_\theta}{\partial r}\frac{\partial u_\theta}{\partial z} + \frac{\partial u_z}{\partial r}\frac{\partial u_z}{\partial z} \tag{1f}$$

where u_r, u_θ and u_z are the displacements in r, θ and z directions, respectively; and ϵ_r, ϵ_θ and ϵ_z are the normal strains; and $\gamma_{r\theta}$, $\gamma_{\theta z}$ and γ_{zr} are the shear strains.

2.3 *Displacement components for curved members with thin-walled open sections*

Consider a thin-walled open crosssection shown in Fig. 2. In the following derivation, two coordinate systems are used to describe the location of a point on the member. The first is the cylindrical coordinate system (x, y, θ) whose origin is taken arbitrarily at point O. The other is the curvilinear coordinate system (n, s, θ) used to describe a point on the section, where s is taken along the middle surface of the thin wall, and n is normal to it, with the origin selected at D. The orientations of these two systems follow the right hand rule. Therefore, the general strain-displacement relations eqn (1) can be written in the following form, as referred to the (x, y, θ) coordinate system.

$$\epsilon_x = \frac{\partial u}{\partial x} + \frac{1}{2}\left[\left(\frac{\partial u}{\partial x}\right)^2 + \left(\frac{\partial v}{\partial x}\right)^2 + \left(\frac{\partial w}{\partial x}\right)^2\right] \tag{2a}$$

$$\epsilon_\theta = \frac{1}{r}\frac{\partial w}{\partial \theta} + \frac{u}{r} + \frac{1}{2r^2}\left[\left(\frac{\partial u}{\partial \theta} - w\right)^2 + \left(\frac{\partial w}{\partial \theta} + u\right)^2 + \left(\frac{\partial v}{\partial \theta}\right)^2\right] \tag{2b}$$

$$\epsilon_y = \frac{\partial v}{\partial y} + \frac{1}{2}\left[\left(\frac{\partial u}{\partial y}\right)^2 + \left(\frac{\partial v}{\partial y}\right)^2 + \left(\frac{\partial w}{\partial y}\right)^2\right] \tag{2c}$$

$$\gamma_{x\theta} = \frac{1}{r}\frac{\partial u}{\partial \theta} - \frac{w}{r} + \frac{\partial w}{\partial x} + \frac{1}{r}\frac{\partial u}{\partial x}\frac{\partial u}{\partial \theta} - \frac{w}{r}\frac{\partial u}{\partial x} + \frac{1}{r}\frac{\partial w}{\partial x}\frac{\partial w}{\partial \theta} + \frac{u}{r}\frac{\partial w}{\partial x} + \frac{1}{r}\frac{\partial v}{\partial x}\frac{\partial v}{\partial \theta} \tag{2d}$$

$$\gamma_{y\theta} = \frac{\partial w}{\partial y} + \frac{1}{r}\frac{\partial v}{\partial \theta} + \frac{1}{r}\frac{\partial u}{\partial y}\frac{\partial u}{\partial \theta} - \frac{w}{r}\frac{\partial u}{\partial y}\frac{\partial w}{\partial \theta} + \frac{u}{r}\frac{\partial w}{\partial y} + \frac{1}{r}\frac{\partial v}{\partial y}\frac{\partial v}{\partial \theta} \tag{2e}$$

$$\gamma_{xy} = \frac{\partial u}{\partial y} + \frac{\partial v}{\partial x} + \frac{\partial u}{\partial x}\frac{\partial u}{\partial y} + \frac{\partial v}{\partial x}\frac{\partial v}{\partial y} + \frac{\partial w}{\partial x}\frac{\partial w}{\partial y} \tag{2f}$$

where u, v and w denote the displacements in x, y and θ directions, respectively. In view of the assumption (1), it is obvious that u and v are much larger than w; hence all the non-linear terms

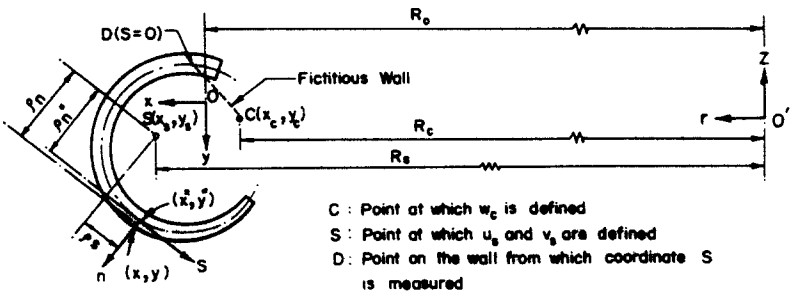

Fig. 2. Cross section of curved members and coordinate systems.

which contain $(\partial w/\partial x)$, $(\partial w/\partial y)$ and $(\partial w/\partial \theta)$ can be neglected in eqns (2) and thus eqns (2) can be reduced to the following form:

$$\epsilon_x = \frac{\partial u}{\partial x} + \frac{1}{2}\left[\left(\frac{\partial u}{\partial x}\right)^2 + \left(\frac{\partial v}{\partial x}\right)^2\right] \tag{3a}$$

$$\epsilon_\theta = \frac{1}{r}\frac{\partial w}{\partial \theta} + \frac{u}{r} + \frac{1}{2r^2}\left[\left(\frac{\partial u}{\partial \theta} - w\right)^2 + u^2 + \left(\frac{\partial v}{\partial \theta}\right)^2\right] \tag{3b}$$

$$\epsilon_y = \frac{\partial v}{\partial y} + \frac{1}{2}\left[\left(\frac{\partial u}{\partial y}\right)^2 + \left(\frac{\partial v}{\partial y}\right)^2\right] \tag{3c}$$

$$\gamma_{x\theta} = \frac{1}{r}\frac{\partial u}{\partial \theta} - \frac{w}{r} + \frac{\partial w}{\partial x} + \frac{1}{r}\frac{\partial u}{\partial x}\frac{\partial u}{\partial \theta} - \frac{w}{r}\frac{\partial u}{\partial x} + \frac{1}{r}\frac{\partial v}{\partial x}\frac{\partial v}{\partial \theta} \tag{3d}$$

$$\gamma_{y\theta} = \frac{\partial w}{\partial y} + \frac{1}{r}\frac{\partial v}{\partial \theta} + \frac{1}{r}\frac{\partial u}{\partial y}\frac{\partial u}{\partial \theta} - \frac{w}{r}\frac{\partial u}{\partial y} + \frac{1}{r}\frac{\partial v}{\partial y}\frac{\partial v}{\partial \theta} \tag{3e}$$

$$\gamma_{xy} = \frac{\partial u}{\partial y} + \frac{\partial v}{\partial x} + \frac{\partial u}{\partial x}\frac{\partial u}{\partial y} + \frac{\partial v}{\partial x}\frac{\partial v}{\partial y}. \tag{3f}$$

The assumption (3) can be expressed mathematically as

$$\epsilon_x = 0, \quad \epsilon_y = 0, \quad \gamma_{xy} = 0. \tag{4}$$

Applying these conditions into eqns (3a), (3c) and (3f) and integrating respectively, lead to the following two expressions for u and v;

$$u = u_s - (y - y_s)\sin\beta - (x - x_s)(1 - \cos\beta) \tag{5a}$$

$$v = v_s + (x - x_s)\sin\beta - (y - y_s)(1 - \cos\beta) \tag{5b}$$

where u_s, v_s and β are the integration constants which can be explained physically as the displacements of an arbitrary reference point $S(x_s, y_s)$ in the x and y directions and the rotation about the axis normal to the plane of S in the anti-clockwise direction to be positive, respectively.

The normal and tangential displacement components ξ and η in the curvilinear coordinate axes n and s are related to u_s and v_s by the following equations;

$$\begin{aligned}\xi &= lu + mv \\ &= lu_s + mv_s - \rho_s \sin\beta - \rho_n(1 - \cos\beta)\end{aligned} \tag{6a}$$

$$\begin{aligned}\eta &= -mu + lv \\ &= -mu_s + lv_s + \rho_n \sin\beta - \rho_s(1 - \cos\beta)\end{aligned} \tag{6b}$$

where l and m are the direction cosines which can be expressed as

$$l = \cos(n, x) = \frac{\partial x}{\partial n} = \frac{\partial y}{\partial s} \tag{7a}$$

$$m = \cos(n, y) = \frac{\partial y}{\partial n} = -\frac{\partial x}{\partial s}. \tag{7b}$$

The quantities ρ_s and ρ_n are the distances between any point on the cross section and the reference point S in the s and n directions, respectively (Fig. 2), and are given by

$$\rho_s = -(x - x_s)m + (y - y_s)l \tag{7c}$$

$$\rho_n = (x - x_s)l + (y - y_s)m. \tag{7d}$$

Similarly, the shear strains on any surface parallel to the middle surface of the wall, $\gamma_{\theta s}$, and those on the planes normal to the middle surface, $\gamma_{\theta n}$, are related to the shear strains $\gamma_{\theta x}$ and $\gamma_{\theta y}$ in the (x, y, θ) coordinate system by

$$\gamma_{\theta s} = l\gamma_{\theta y} - m\gamma_{\theta x} \tag{8a}$$

$$\gamma_{\theta n} = l\gamma_{\theta x} + m\gamma_{\theta y}. \tag{8b}$$

In view of eqns (3d), (3f), (6) and (7), eqns (8) can be expressed in the following form:

$$\gamma_{\theta s} = r\frac{\partial}{\partial s}\left(\frac{w}{r}\right) - \frac{w}{r}\frac{\partial u}{\partial s} + \frac{1}{r}\frac{\partial u}{\partial \theta}\frac{\partial u}{\partial s} + \frac{1}{r}\frac{\partial v}{\partial \theta}\frac{\partial v}{\partial s} + \frac{1}{r}\frac{\partial \eta}{\partial \theta} \tag{9a}$$

$$\gamma_{\theta n} = r\frac{\partial}{\partial n}\left(\frac{w}{r}\right) - \frac{w}{r}\frac{\partial u}{\partial n} + \frac{1}{r}\frac{\partial u}{\partial \theta}\frac{\partial u}{\partial n} + \frac{1}{r}\frac{\partial v}{\partial \theta}\frac{\partial v}{\partial n} + \frac{1}{r}\frac{\partial \xi}{\partial \theta}. \tag{9b}$$

Since open cross sections are considered in this study, the assumptions (4) and (5) can be interpreted as

$$\gamma_{\theta n} = 0 \tag{10a}$$

$$\gamma^*_{\theta s} = 0 \tag{10b}$$

where $(\ )^*$ denotes the quantity defined along the middle line (i.e. $n = 0$). By using eqns (5), (6) and (9), eqns (10) will lead to the following two differential equations;

$$r\frac{\partial}{\partial n}\left(\frac{w}{r}\right) + [m\sin\beta + l(1-\cos\beta)]\frac{w}{r} = \frac{1}{r}[(u'_s m - v'_s l)\sin\beta - (u'_s l + v'_s m)\cos\beta + \rho_s\beta'] \tag{11a}$$

$$r^*\frac{\partial}{\partial s}\left(\frac{w^*}{r^*}\right) + [l^*\sin\beta - m^*(1-\cos\beta)]\frac{w^*}{r^*} = \frac{1}{r^*}[(u'_s l^* + v'_s m^*)\sin\beta - (-u'_s m^* + v'_s l^*)\cos\beta - \rho^*_n\beta'] \tag{11b}$$

where prime indicates differentiation with respect to θ. Solving the first differential equation (11a) yields

$$w = w^*\left(\frac{r^*}{r}\right)^{(m/l)\sin\beta - \cos\beta} + \frac{1}{m\sin\beta - l\cos\beta}\left[1 - \left(\frac{r^*}{r}\right)^{(m/l)\sin\beta - \cos\beta}\right] \times [(u'_s m - v'_s l)\sin\beta - (u'_s l + v'_s m)\cos\beta + \rho_s\beta']. \tag{12}$$

The exponential terms in eqn (12) can be expressed in the following form of binomal series:

$$\left(\frac{r^*}{r}\right)^{(m/l)\sin\beta - \cos\beta} = \left(1 + \frac{r - r^*}{r^*}\right)^{-(m/l)\sin\beta + \cos\beta}$$

$$= 1 + \left(-\frac{m}{l}\sin\beta + \cos\beta\right)\frac{r - r^*}{r^*} + \frac{1}{2}\left(-\frac{m}{l}\sin\beta + \cos\beta\right) \times \left(-\frac{m}{l}\sin\beta + \cos\beta - 1\right)\left(\frac{r - r^*}{r^*}\right)^2 + \cdots\cdots \tag{13}$$

It is obvious that the value of $(r - r^*)/r^*$ is very small for curved members with thin-walled section; therefore, eqn (13) can be reasonably approximated in the following way,

$$\left(\frac{r^*}{r}\right)^{(m/l)\sin\beta - \cos\beta} = 1 - \left(\frac{m}{l}\sin\beta - \cos\beta\right)\frac{r - r^*}{r^*}. \tag{14}$$

Using eqn (14) and the following geometric relations

$$x - x^* = r - r^* = nl \tag{15a}$$

$$y - y^* = nm \tag{15b}$$

$$\rho_n = \rho_n^* + n \tag{15c}$$

$$\rho_n^* = (x^* - x_s)l + (y^* - y_s)m \tag{15d}$$

$$\rho_s^* = -(x^* - x_s)m + (y^* - y_s)l. \tag{15e}$$

Equation (12) can be simplified into the following form

$$w = w^* + \frac{x - x^*}{r^*}\left(w^* \cos\beta - v_s' \sin\beta - u_s' \cos\beta\right) + \frac{y - y^*}{r^*}$$

$$\times(-w^* \sin\beta + u_s' \sin\beta - v_s' \cos\beta) + \frac{n\rho_s}{r^*}\beta'. \tag{16}$$

It is to be noted that the same equation is obtainable by replacing w in the second term of the left hand side of eqn (11a) by w^* and by integrating it. Similarly, the solution of eqn (11b) is approximately given by

$$w^* = w_c - \frac{x^* - x_c}{R_c}\left[-w_c \cos\beta + v_s' \sin\beta + u_s' \cos\beta - (-w_c \sin\beta + u_s' \sin\beta - v_s' \cos\beta)\frac{y_s - y_c}{R_s}\right]$$

$$+(-w_c \sin\beta + u_s' \sin\beta - v_s' \cos\beta)\frac{y^* - y_c}{R_s}$$

$$-\omega^*\left(\frac{-w_c \sin\beta + u_s' \sin\beta - v_s' \cos\beta}{R_s^2} + \frac{\beta'}{R_s}\right) \tag{17}$$

where w_c = displacement w defined at a reference point $C(x_c, y_c)$ on the corss section (Fig. 2), R_s, R_c = radii of curvature of points S and C, respectively, and

$$\omega^* = \Omega^* - \frac{r^*}{R_c}\Omega_c^* \tag{18a}$$

$$\Omega^* = R_s r^* \int_0^s \frac{1}{r^{*2}}\rho_n^* \, ds \tag{18b}$$

$$\Omega_c^* = R_s R_c \int_0^{s_c} \frac{1}{r^{*2}}\rho_n^* \, ds. \tag{18c}$$

Since the reference point $C(x_c, y_c)$ does not generally lie on the thin wall, in order to relate the displacement in θ direction in terms of point C, an arbitrary fictitious thin wall is introduced to connect point C and D as shown in Fig. 2[11]. This segment CD is considered to be infinitesimally thin and it would not alter the characteristic of the thin-wall member. The quantity s_c in eqn (18c) is designated to be the distance from C to D along the fictitious wall.

Substituting eqn (17) into eqn (16), leads to the following expression for w

$$w = w_c - \frac{x - x_c}{R_c}\left(f - g\frac{y_s - y_c}{R_s}\right) + \frac{y - y_c}{R_s}g - \omega\left(\frac{g}{R_s^2} + \frac{\beta'}{R_s}\right) \tag{19}$$

where

$$f = (u_s' - w_c)\cos\beta + v_s' \sin\beta \tag{20a}$$

$$g = (u_s' - w_c)\sin\beta - v_s' \cos\beta \tag{20b}$$

$$\omega = \frac{r}{r^*}\Omega^* - \frac{R_s}{r^*} n\rho_s - \frac{r}{R_c}\Omega_c^*. \tag{20c}$$

The quantity ω denotes the unit warping[1].

2.4 *Strain-displacement relations*

In view of eqn (4) and (10a), the six strains components in eqns (3) have already been reduced to only two non-vanishing components namely ϵ_θ and $\gamma_{\theta s}$, which can be obtained by substituting all the three displacements eqns (5) and (19) into eqn (3b) and (9a), as given in the following:

$$\begin{aligned}\epsilon_\theta = {} & \frac{w_c'}{r} - \frac{x-x_c}{r}\left(\frac{f'}{R_c} - \frac{g'}{R_c}\frac{y_s-y_c}{R_s}\right) + \frac{y-y_c}{r}\frac{g'}{R_s} - \frac{\omega}{r}\left(\frac{g'}{R_s^2} + \frac{\beta''}{R_s}\right) \\ & + \frac{1}{r}[u_s - (y-y_s)\sin\beta - (x-x_s)(1-\cos\beta)] \\ & + \frac{1}{2r^2}\Big[u_s' - (y-y_s)\beta'\cos\beta - (x-x_s)\beta'\sin\beta - w_c \\ & + \frac{x-x_c}{R_c}\left(f - g\frac{y_s-y_c}{R_s}\right) \\ & - \frac{y-y_c}{R_s}g + \omega\left(\frac{g}{R_s^2} + \frac{\beta'}{R_s}\right)\Big]^2 + \frac{1}{2r^2}[u_s - (y-y_s)\sin\beta \\ & - (x-x_s)(1-\cos\beta)]^2 \\ & + \frac{1}{2r^2}[v_s' + (x-x_s)\beta'\cos\beta - (y-y_s)\beta'\sin\beta]^2 \end{aligned} \tag{21a}$$

$$\gamma_{\theta s} = \frac{R_s^2 n}{rr^*}\left(2 + \frac{nl}{r^*}\right)\left(\frac{g}{R_s^2} + \frac{\beta'}{R_s}\right). \tag{21b}$$

These are the general expressions for the non-vanishing strain components of thin-walled curved members. It is to be noted that the point S and C can be selected arbitrarily in these expressions.

Now, two special cases are considered here. Firstly, if the problem is restricted to be small displacement theory, all the non-linear terms may be omitted. Thus, by using the approximations,

$$\cos\beta \simeq 1.0, \quad \sin\beta \simeq \beta \tag{22}$$

the following expressions for ϵ_θ and $\gamma_{\theta s}$ can be obtained.

$$\begin{aligned}\epsilon_\theta = {} & \frac{R_s}{r}\left\{\left(\frac{w_c'}{R_s} + \frac{u_s}{R_s} + \frac{y_s-y_c}{R_s}\beta - (x-x_c)\frac{R_s}{R_c}\left(\frac{u_s''}{R_s^2} + \frac{y_s-y_c}{R_s}\frac{v_s''}{R_s^2} - \frac{w_c'}{R_s^2}\right)\right.\right. \\ & \left.\left. - (y-y_c)\left(\frac{v_s''}{R_s^2} + \frac{\beta}{R_s}\right) - \omega\left(\frac{\beta''}{R_s^2} - \frac{v_s''}{R_s^3}\right)\right\} \end{aligned} \tag{23a}$$

$$\gamma_{\theta s} = \frac{R_s^2 n}{rr^*}\left(2 + \frac{nl}{r^*}\right)\left(\frac{\beta'}{R_s} - \frac{v_s'}{R_s^2}\right). \tag{23b}$$

These two expressions are exactly the same as those derived by Nishino *et al.*[11]. Furthermore, if points C and S are selected to be coincident with the origin O (i.e. $x_c = y_c = x_s = y_s = 0$) and the difference of radius of curvature over the cross section is neglected (i.e. $r = R_s = R_c$), then eqns (23) can be reduced to the expressions which were obtained by Vlasov[1]. Secondly, if the curved member is specialized into a straight member and point C is selected to be the origin O (i.e. $x_c = y_c = 0$), eqns (21) can be reduced to the following expressions by putting

$dz = r\,d\theta$ and by making r, R_s and R_c approaching infinite;

$$\epsilon_\theta = \epsilon_z = w_c' + \frac{1}{2}(u_s'^2 + v_s'^2) + \Big\{(y_s u_s' - x_s v_s')\cos\beta + (x_s u_s' + y_s v_s')\sin\beta\Big\}\beta' - x(v_s''\sin\beta + u_s''\cos\beta) - y(-u_s''\sin\beta + v_s''\cos\beta) - \omega\beta'' + \frac{1}{2}\{(x - x_s)^2 + (y - y_s)^2\}\beta'^2 \tag{24a}$$

$$\gamma_{\theta s} = \gamma_{zs} = 2n\beta' \tag{24b}$$

where prime indicates differentiation with respect to z. These are again exactly the same as those obtained by Nishino *et al.*[20].

2.5 *Governing differential equations for equilibrium and its associated boundary conditions*

The governing differential equations for equilibrium and the associated boundary conditions for curved members can be established on the basis of selecting two reference points S and C arbitrarily. However, in this section, point C is selected to be coincident with point S because this gives the simplest form of the governing differential equations for equilibrium and the associated boundary conditions.

Consider the free body of a curved member which is in equilibrium condition under the applied distributed external loadings $\bar{\mathbf{P}}$ and the applied external stresses $\bar{\mathbf{f}}$ at both ends of the member. By the principle of virtual work[15]

$$\int_{\theta_1}^{\theta_2}\int_A (\sigma_\theta \delta\epsilon_\theta + \tau_{\theta s}\delta\gamma_{\theta s})\,dA r\,d\theta = \int_{\theta_1}^{\theta_2}\int_A \bar{\mathbf{P}}\delta\mathbf{r}\,dA r\,d\theta + \Big[\nu_\theta \int_A \bar{\mathbf{f}}\delta\mathbf{r}\,dA\Big]_{\theta_1}^{\theta_2} \tag{25}$$

where

$$\bar{\mathbf{P}} = \bar{p}_x\mathbf{i}_x + \bar{p}_y\mathbf{i}_y + \bar{p}_\theta\mathbf{i}_\theta \tag{26a}$$

$$\bar{\mathbf{f}} = \bar{\tau}_{\theta n}\mathbf{i}_n + \bar{\tau}_{\theta s}\mathbf{i}_s + \bar{\sigma}_\theta\mathbf{i}_\theta \tag{26b}$$

$$\mathbf{r} = u\mathbf{i}_x + v\mathbf{i}_y + w\mathbf{i}_\theta = \xi\mathbf{i}_n + \eta\mathbf{i}_s + w\mathbf{i}_\theta \tag{26c}$$

$$\nu_\theta = 1 \quad \text{at} \quad \theta = \theta_2 \qquad = -1 \quad \text{at} \quad \theta = \theta_1. \tag{26d}$$

Here, $\mathbf{i}_x$, $\mathbf{i}_y$, $\mathbf{i}_\theta$ are the unit vectors in the cylindrical coordinate system (x, y, θ); $\mathbf{i}_n$, $\mathbf{i}_s$, $\mathbf{i}_\theta$ are the unit vectors in curvilinear coordinate system (n, s, θ); and θ_1 and θ_2 are the values of θ at both ends of the members. Substituting eqns (5), (6), (19) and (21) into the virtual work equation (25) and introducing the following terms

$$\bar{q}_x = \int_A \frac{r}{R_s}\bar{p}_x\,dA \tag{27a}$$

$$\bar{q}_y = \int_A \frac{r}{R_s}\bar{p}_y\,dA \tag{27b}$$

$$\bar{q}_\theta = \int_A \frac{r}{R_s}\bar{p}_\theta\,dA \tag{27c}$$

$$\bar{m}_x = \int_A \frac{r}{R_s}\bar{p}_\theta(y - y_s)\,dA \tag{27d}$$

$$\bar{m}_y = \int_A \frac{r}{R_s}\bar{p}_\theta(x - x_s)\,dA \tag{27e}$$

$$\bar{m}_{\omega} = \int_A \frac{r}{R_s} \bar{p}_{\theta}\omega \, \mathrm{d}A \tag{27f}$$

$$\bar{m}_{xy} = \int_A \frac{r}{R_s} [\bar{p}_x(x - x_s) + \bar{p}_y(y - y_s)] \, \mathrm{d}A \tag{27g}$$

$$\bar{m}_{\theta} = \int_A \frac{r}{R_s} [\bar{p}_y(x - x_s) - \bar{p}_x(y - y_s)] \, \mathrm{d}A \tag{27h}$$

$$\bar{N} = \int_A \bar{\sigma}_{\theta} \, \mathrm{d}A \tag{27i}$$

$$\bar{M}_x = \int_A \bar{\sigma}_{\theta} y \, \mathrm{d}A \tag{27j}$$

$$\bar{M}_y = \int_A \bar{\sigma}_{\theta} x \, \mathrm{d}A \tag{27k}$$

$$\bar{M}_{\omega} = \int_A \bar{\sigma}_{\theta}\omega \, \mathrm{d}A \tag{27l}$$

$$\bar{Q}_x = \int_A (-m\bar{\tau}_{\theta s} + l\bar{\tau}_{\theta n}) \, \mathrm{d}A \tag{27m}$$

$$\bar{Q}_y = \int_A (l\bar{\tau}_{\theta s} + m\bar{\tau}_{\theta n}) \, \mathrm{d}A \tag{27n}$$

$$\bar{T}_{xy} = \int_A (\bar{\tau}_{\theta s}\rho_s + \bar{\tau}_{\theta n}\rho_n) \, \mathrm{d}A \tag{27o}$$

$$\bar{T} = \int_A (\bar{\tau}_{\theta s}\rho_n - \bar{\tau}_{\theta n}\rho_s) \, \mathrm{d}A \tag{27p}$$

$$N = \int_A \sigma_{\theta} \, \mathrm{d}A \tag{28a}$$

$$M_x = \int_A \sigma_{\theta} y \, \mathrm{d}A \tag{28b}$$

$$M_y = \int_A \sigma_{\theta} x \, \mathrm{d}A \tag{28c}$$

$$M_{\omega} = \int_A \sigma_{\theta}\omega \, \mathrm{d}A \tag{28d}$$

$$\tilde{N} = \int_A \frac{R_s}{r} \sigma_{\theta} \, \mathrm{d}A \tag{28e}$$

$$\tilde{M}_x = \int_A \frac{R_s}{r} \sigma_{\theta} y \, \mathrm{d}A \tag{28f}$$

$$\tilde{M}_y = \int_A \frac{R_s}{r} \sigma_{\theta} x \, \mathrm{d}A \tag{28g}$$

$$\tilde{M}_{\omega} = \int_A \frac{R_s}{r} \sigma_{\theta}\omega \, \mathrm{d}A \tag{28h}$$

$$K_x = \int_A \frac{R_s}{r} \sigma_{\theta}(x - x_s)^2 \, \mathrm{d}A \tag{28i}$$

$$K_y = \int_A \frac{R_s}{r} \sigma_{\theta}(y - y_s)^2 \, \mathrm{d}A \tag{28j}$$

$$K_{xy} = \int_A \frac{R_s}{r} \sigma_{\theta}(x - x_s)(y - y_s) \, \mathrm{d}A \tag{28k}$$

$$K_\omega = \int_A \frac{R_s}{r} \sigma_\theta \omega^2 \, dA \tag{28l}$$

$$K_{\omega x} = \int_A \frac{R_s}{r} \sigma_\theta \omega (x - x_s) \, dA \tag{28m}$$

$$K_{\omega y} = \int_A \frac{R_s}{r} \sigma_\theta \omega (y - y_s) \, dA \tag{28n}$$

$$M_{SV} = \int_A \tau_{\theta s} \frac{R_s n}{r^*} \left(2 + \frac{nl}{r^*}\right) dA \tag{28o}$$

and integrating by parts, leads to four governing differential equations for equilibrium and associated boundary conditions which are shown in Appendix 1.

2.6 *Force-displacement relations*

For this one-dimensional theory, the stresses are directly related to the corresponding strains by the modulus of elasticity E and shear modulus G of an elastic material. Hence,

$$\sigma_\theta = E\epsilon_\theta \tag{29a}$$

$$\tau_{\theta s} = G\gamma_{\theta s}. \tag{29b}$$

Substituting eqns (21) and (29) into eqns (28) yields the force-displacement relations of curved members. Since the expressions are rather complex, only the linear parts of the relations are shown in Appendix 2.

Now, in order to express the linear force-displacement relations, the following properties of cross section must be defined.

$$A = \int_A \frac{R_0}{r} dA \tag{30a}$$

$$Z_x = \int_A \frac{R_0}{r} y \, dA \tag{30b}$$

$$Z_y = \int_A \frac{R_0}{r} x \, dA \tag{30c}$$

$$I_x = \int_A \frac{R_0}{r} y^2 \, dA \tag{30d}$$

$$I_y = \int_A \frac{R_0}{r} x^2 \, dA \tag{30e}$$

$$I_{xy} = \int_A \frac{R_0}{r} xy \, dA \tag{30f}$$

$$Z_\omega = \int_A \frac{R_S}{r} \omega \, dA \tag{30g}$$

$$I_{\omega y} = \int_A \frac{R_S}{r} \omega y \, dA \tag{30h}$$

$$I_{\omega x} = \int_A \frac{R_S}{r} \omega x \, dA \tag{30i}$$

$$I_\omega = \int_A \frac{R_S}{r} \omega^2 \, dA \tag{30j}$$

$$K_T = \int_A \frac{R_s}{r} \frac{R_s^2 n^2}{r^{*2}} \left(2 + \frac{nl}{r^*}\right)^2 dA. \tag{30k}$$

As mentioned by Vlasov[1], by setting

$$Z_x = \int_A \frac{R_0}{r} y \, dA = 0 \tag{31a}$$

$$Z_y = \int_A \frac{R_0}{r} x \, dA = 0 \tag{31b}$$

the coordinate origin O in Fig. 2 can be located; and by putting

$$Z_\omega = \int_A \frac{R_s}{r} \omega \, dA = 0 \tag{31c}$$

the position of the origin of s which is the D point in Fig. 2 can be found; and by using the following two equations

$$I_{\omega x} = \int_A \frac{R_s}{r} \omega x \, dA = 0 \tag{31d}$$

$$I_{\omega y} = \int_A \frac{R_s}{r} \omega y \, dA = 0 \tag{31e}$$

the position of the S point, which is usually called the shear center, can be found.

3. APPLICATION—LATERAL-TORSIONAL BUCKLING OF CIRCULAR ARCHES WITH THIN-WALLED OPEN SECTIONS

3.1 *Introduction*

The large displacement theory of curved members developed in the previous chapter is applied to lateral-torsional buckling analysis of circular arches in this chapter. When a planar arch is subjected to a system of loading in its plane, it may buckle out of its plane. This phenomenon is analogous to the lateral-torsional buckling of straight members[21]. The lateral-torsional buckling analysis of arches and rings has been investigated by numerous authors. An excellent summary of those studies is given in Ref.[22]. However, as pointed out in this reference, most of the previous investigators have neglected the effect of warping torsional rigidity in their analyses, and only a few studies have been published in which the warping effects are taken into consideration[1, 4, 12, 23–26]. Furthermore, except for Cheney[4], all the investigators have formulated the equations without considering the difference in the radius of curvature of the member over the cross section.

In this study, a general virtual work equation, which governs the lateral-torsional buckling of arches and ring segments subjected to an arbitrary system of in-plane loading, will be derived. This derived equation is linearlized with respect to out-of-plane displacements, but stresses and displacements at the pre-buckling state are considered to be finite quantities. Thus, the effects of in-plane deformations on the lateral-torsional buckling analysis can be evaluated through this analysis.

3.2 *Derivation of general form of virtual work equation*

Beside the assumptions made in the Section 2, the following additional assumptions are made in the present analysis: (1) The arch is of a mono-symmetric thin-walled open section with its symmetric axis laying in the plane of the arch. (2) Prior to buckling, applied loads act in the plane of the arch and thus the arch deforms in its plane only. (3) During buckling, applied loads remain fixed in magnitude and direction, but move perpendicularly to the plane of the arch. (4) In-plane displacements, strains and stresses are finite, but out-of-plane displacements, strains and stresses are infinitesimally small. (5) No in-plane buckling is considered.

Consider a mono-symmetric crossection shown in Fig. 3(a). The points O, S and D are chosen in such a way that eqns (31) are all satisfied. The point C is taken as the same as point S. Due to the symmetry of the cross section, the points O and S i.e. on the x-axis.

In view of the assumption (4), the in-plane displacements are of finite magnitude, i.e.

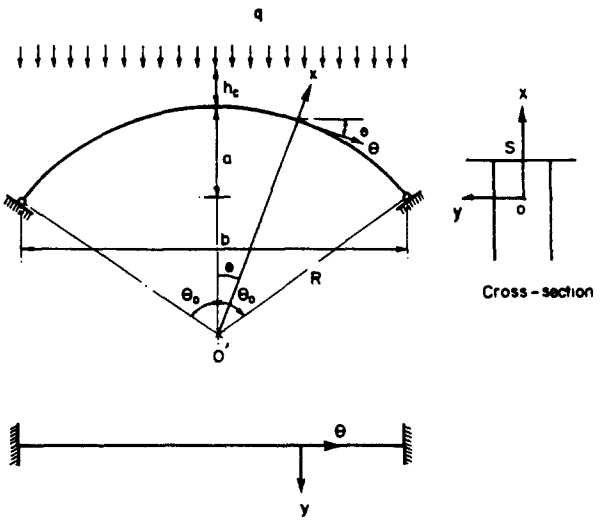

Fig. 3. Circular arch with uniformly distributed load.

u_s, $w_s = O(1)$, and the out-of-plane displacements are of infinitesimal magnitude, i.e. v_s, $\beta = O(\epsilon)$ (where ϵ denotes an infinitesimal magnitude). Introducing this assumption to the strain-displacement relations eqns (21) and neglecting terms higher than $O(\epsilon^2)$ result in the following expressions;

$$\epsilon_\theta = \frac{w_s' + u_s}{r} - \frac{x - x_s}{r}\left(\frac{f'}{R_s} + \frac{\beta^2}{2}\right) + \frac{y}{r}\left(\frac{g'}{R_s} - \beta\right) - \frac{\omega}{r}\left(\frac{g'}{R_s^2} + \frac{\beta''}{R_s}\right)$$
$$+ \frac{1}{2r^2}\left\{u_s' - w_s + (x - x_s)\left(\frac{f}{R_s} - \beta\beta'\right) - y\left(\frac{g}{R_s} + \beta'\right) + \omega\left(\frac{g}{R_s^2} + \frac{\beta'}{R_s}\right)\right\}^2$$
$$+ \frac{1}{2r^2}\left\{u_s - y\beta - (x - x_s)\frac{\beta_2}{2}\right\}^2 + \frac{1}{2r^2}\{v_s' + (x - x_s)\beta' - y\beta\beta'\}^2 \tag{32a}$$

$$\gamma_{\theta s} = \frac{R_s^2 n}{rr^*}\left(2 + \frac{nl}{r^*}\right)\left(\frac{g}{R_s^2} + \frac{\beta'}{R_s}\right) \tag{32b}$$

where

$$f = (u_s' - w_s)\left(1 - \frac{\beta^2}{2}\right) + v_s'\beta \tag{33a}$$

$$g = (u_s' - w_s)\beta - v_s'. \tag{33b}$$

In deriving eqns (32) we have used $y_c = y_s = 0$, $R_c = R_s$, $x_c = x_s$ and $w_c = w_s$.

Next, we shall formulate the virtual work equation of arches just after buckling based on the strain-displacement relation (32). In the following description, the superscript (0) is used to denote displacement, strain and force parameters just before buckling, and when these parameters appear without the superscript, they refer to the incremental values from prebuckling to post-buckling states. Owing to the assumption (4), the incremental values are of $O(\epsilon)$. Now, the virtual work equation after buckling can be written in the form[15];

$$\int_{\theta_1}^{\theta_2}\int_A \{(\sigma_\theta^{(0)} + \sigma_\theta)\delta(\epsilon_\theta^{(0)} + \epsilon_\theta) + (\tau_{\theta s}^{(0)} + \tau_{\theta s})\delta(\gamma_{\theta s}^{(0)} + \gamma_{\theta s})\}\,dA r\,d\theta$$
$$= \int_{\theta_1}^{\theta_2}\{\bar{q}_x^{(0)}\delta(u_p^{(0)} + u_p) + \bar{q}_\theta^{(0)}\delta(w_p^{(0)} + w_p)\}R_s\,d\theta \tag{34}$$

where u_p and w_p are, respectively, displacement components u and w at the point of

applciation of external forces. Here, we have assumed that no external forces act at the ends of members. It is to be noted that, in view of assumption (2), the increments of in-plane forces $\bar{q}_x$ and $\bar{q}_\theta$ are zero. Stability analysis based on eqn (34) is called the Euler method[15]. Replacing u_s, w_s, ϵ_θ and $\gamma_{\theta s}$ in eqns (32) by $u_s^{(0)}+u_s$, $w_s^{(0)}+w_s$, $\epsilon_\theta^{(0)}+\epsilon_\theta$ and $\gamma_{\theta s}^{(0)}+\gamma_{\theta s}$, respectively, leads to the following expressions for variations in the strain components;

$$\delta(\epsilon_\theta^{(0)}+\epsilon_\theta)=\delta\epsilon_{I1}+\delta\epsilon_{I2}+\delta\epsilon^{\mathcal{L}}+\delta\epsilon^{\mathcal{NL}} \tag{35a}$$

$$\delta(\gamma_{\theta s}^{(0)}+\gamma_{\theta s})=\delta\gamma_{I1}+\delta\gamma_{I2}+\delta\gamma^{\mathcal{L}}+\delta\gamma^{\mathcal{NL}}. \tag{35b}$$

Here

$$\delta\epsilon_{I1}=\frac{\delta(w_s'+u_s)}{r}-\frac{x-x_s}{r}\frac{\delta(u_s''-w_s')}{R_s}+\frac{(u_s'-w_s+d^{(0)})\delta(u_s'-w_s)}{R_s^2}+\frac{u_s+u_s^{(0)}}{r^2}\delta u_s \tag{36a}$$

$$\delta\epsilon_{I2}=\frac{1}{R_s r}\left(y-\frac{\omega}{R_s}\right)\delta\{(u_s'-w_s)\beta\}'-\frac{1}{R_s^2 r}\left(y-\frac{\omega}{R_s}\right)\delta\{(d^{(0)}\beta-v_s'+R_s\beta')(u_s'-w_s)\}-\frac{y}{r^2}\delta(u_s\beta) \tag{36b}$$

$$\delta\epsilon^{\mathcal{L}}=\frac{y}{R_s r}\left\{(d^{(0)}\delta\beta)'-\delta v_s''-R_s\left(1+\frac{u_s^{(0)}}{r}\right)\delta\beta\right\}-\frac{\omega}{R_s^2 r}\{(d^{(0)}\delta\beta)'-\delta v_s''+R_s\delta\beta''\}-\frac{1}{R_s^2 r}\left(y-\frac{\omega}{R_s}\right)d^{(0)}(d^{(0)}\delta\beta-\delta v_s'+R_s\delta\beta') \tag{36c}$$

$$\delta\epsilon^{\mathcal{NL}}=-\frac{x-x_s}{R_s r}\left\{\delta(v_s'\beta)'-d^{(0)\prime}\beta\delta\beta+\frac{d^{(0)}}{R_s}[d^{(0)}\beta\delta\beta-\delta(v_s'\beta)]+R_s\left(1+\frac{u_s^{(0)}}{r}\right)\beta\delta\beta\right\}+\frac{1}{R_s^2 r^2}\left(y-\frac{\omega}{R_s}\right)^2(d^{(0)}\beta-v_s'+R_s\beta')(d^{(0)}\delta\beta-\delta v_s'+R_s\delta\beta')+\frac{y^2}{r^2}\beta\delta\beta+\frac{1}{r^2}[v_s'+(x-x_s)\beta'][\delta v_v'+(x-x_s)\delta\beta'] \tag{36d}$$

$$\delta\gamma_{I1}=0 \tag{36e}$$

$$\delta\gamma_{I2}=\frac{n}{rr^*}\left(2+\frac{nl}{r^*}\right)\delta[(u_s'-w_s)\beta] \tag{36f}$$

$$\delta\gamma^{\mathcal{L}}=\frac{n}{rr^*}\left(2+\frac{nl}{r^*}\right)(d^{(0)}\delta\beta-\delta v_s'+R_s\delta\beta') \tag{36g}$$

$$\delta\gamma^{\mathcal{NL}}=0 \tag{36h}$$

$$d^{(0)}=u_s^{(0)\prime}-w_s^{(0)} \tag{36i}$$

where ϵ_{I1}, γ_{I1} = strain components due to in-plane displacement increments, ϵ_{I2}, γ_{I2} = strain components due to coupled in-plane and out-of-plane displacement increments, $\epsilon^{\mathcal{L}}$, $\gamma^{\mathcal{L}}$ = linear strain components due to out-of-plane displacements, and $\epsilon^{\mathcal{NL}}$, $\gamma^{\mathcal{NL}}$ = non-linear strain components due to out-of-plane displacements. Similarly, the variations in the displacement components at the point of application of external loads can be determined from eqns (5) and eqns (19) as follows:

$$\delta(u_p^{(0)}+u_p)=\delta u_{I1}+\delta u_{I2}+\delta u^{\mathcal{L}}+\delta u^{\mathcal{NL}} \tag{37a}$$

$$\delta(w_p^{(0)}+w_p)=\delta w_{I1}+\delta w_{I2}+\delta w^{\mathcal{L}}+\delta w^{\mathcal{NL}} \tag{37b}$$

where

$$\delta u_{I1}=\delta u_s \tag{38a}$$

$$\delta u_{12} = 0 \tag{38b}$$

$$\delta u^{\mathscr{L}} = 0 \tag{38c}$$

$$\delta u^{\mathscr{NL}} = -(x_p - x_s)\beta\delta\beta \tag{38d}$$

$$\delta w_{11} = \delta w_s - \frac{x_p - x_s}{R_s}\,\delta(u_s' - w_s) \tag{38e}$$

$$\delta w_{12} = -\frac{\omega}{R_s^2}\,\delta\{(u_s' - w_s)\beta\} \tag{38f}$$

$$\delta w^{\mathscr{L}} = -\frac{\omega}{R_s^2}\,\delta(d^{(0)}\beta + R_s\beta') \tag{38g}$$

$$\delta w^{\mathscr{NL}} = -\frac{x_p - x_s}{R_s}\{\delta(v_s'\beta) - d^{(0)}\beta\delta\beta\}. \tag{38h}$$

Here, x_p is the x coordinate of the point of application of external loads. Now, substituting eqns (35) and eqns (37) into the virtual work equation (34) and neglecting terms higher than $O(\epsilon^2)$, we shall obtain

$$\int_{\theta_1}^{\theta_2}\int_A [\sigma_\theta\delta\epsilon^{\mathscr{L}} + \tau_{\theta s}\delta\gamma^{\mathscr{L}} + \sigma_\theta^{(0)}\delta\epsilon^{\mathscr{NL}}]\,\mathrm{d}A r\,\mathrm{d}\theta - \int_{\theta_1}^{\theta_2}(\bar{q}_x^{(0)}\delta u^{\mathscr{NL}} + \bar{q}_\theta^{(0)}\delta w^{\mathscr{NL}})R_s\,\mathrm{d}\theta = 0 \tag{39}$$

where

$$\sigma_\theta = E\epsilon^{\mathscr{L}} \quad \text{and} \quad \tau_{\theta s} = G\gamma^{\mathscr{L}}. \tag{40}$$

In deriving eqn (39), we have used the relation

$$\int_{\theta_1}^{\theta_2}\int_A (\sigma_\theta^{(0)} + \sigma_\theta)\delta\epsilon_{11}\,\mathrm{d}A r\,\mathrm{d}\theta = \int_{\theta_1}^{\theta_2}(\bar{q}_x^{(0)}\delta u_{11} + \bar{q}_\theta^{(0)}\delta w_{11})R_s\,\mathrm{d}\theta \tag{41}$$

and the fact that $\sigma_\theta^{(0)}$ and ω are respectively symmetric and antisymmetric with respect to the x-axis of the cross section. Equation (39) is the most general form of the virtual work equation governing the lateral-torsional buckling of arches with mono-symmetric thin-walled open sections. Particular mention is made herein that, although we did not assume that the increments of in-plane displacements are zero, the resulting virtual work eqn (39) is independent of those quantities. Thus, the same virtual work equation can be obtained by assuming that in-plane displacements do not change during buckling. This assumption will definitely make the formulation of eqn (39) much easier.

Now, if appropriate functions for out-of-plane displacement components are assumed, the lateral-torsional buckling equation of the arch is easily obtained from the virtual work equation (39).

3.3 *Numerical example*

As a numerical example, the circular arch shown in Fig. 3 is considered here. The arch ends are pinned in its plane and fixed out of its plane. The uniformly distributed load q applied along the span is located at the distance of h_c above the crown. The θ coordinate is measured from the crown. To make the analysis simple, the following conditions are used; (1) The radius of curvature of the arch is large as compared with its cross-sectional dimensions so that $r = R_0 = R_s = R$. (2) The crosssection is doubly symmetric so that $x_s = 0$. (3) The in-plane displacements and forces obtained from linear analysis are used for the corresponding quantities just before buclking. (4) Product terms of in-plane displacements (i.e. $d^{(0)2}$ in eqns (36)) are neglected.

Owing to the condition (1), the cross-sectional properties given in eqn (33) become the same as those for straight members. In view of the condition (3), the in-plane forces and displace-

ments are given as

$$N^{(0)} = qR\left[-\frac{1}{2} - \Gamma\cos\theta + \frac{1}{2}\cos 2\theta\right] \tag{42a}$$

$$M_y^{(0)} = qR^2\left[-\Phi_1 + \Gamma\cos\theta - \frac{1}{4}\cos 2\theta\right] \tag{42b}$$

$$u_s^{(0)} = \frac{qR^4}{EI_y}\left[\Phi_1 - \frac{\bar{\kappa}}{2} + \left(\Phi_2 + \frac{1-\bar{\kappa}}{2}\Gamma\right)\cos\theta - \frac{1+\bar{\kappa}}{2}\Gamma\theta\sin\theta - \frac{1+2\bar{\kappa}}{12}\cos 2\theta\right] \tag{42c}$$

$$w_s^{(0)} = \frac{qR^4}{EI_y}\left[-\Phi_1\theta - \Phi_2\sin\theta - \frac{1+\bar{\kappa}}{2}\Gamma\theta\cos\theta + \frac{1+8\bar{\kappa}}{24}\sin 2\theta\right] \tag{42d}$$

$$\Gamma = \frac{3(\theta_0\cos\theta_0\cos 2\theta_0 - \sin\theta_0) + (7-4\bar{\kappa})\sin\theta_0}{6\theta_0(2+\cos 2\theta_0 + \bar{\kappa}) - 3(3-\bar{\kappa})\sin 2\theta_0} \tag{42e}$$

$$\Phi_1 = \frac{1}{4}(4\Gamma\cos\theta_0 - \cos 2\theta_0) \tag{42f}$$

$$\Phi_2 = \frac{1}{12}\left[(1+8\bar{\kappa})\cos\theta_0 - \frac{6\theta_0}{\sin\theta_0}\{2\Phi_1 + (1+\bar{\kappa})\Gamma\cos\theta_0\}\right] \tag{42g}$$

$$\bar{\kappa} = \frac{EI_y}{R^2EA}. \tag{42h}$$

Now, assume that the out-of-plane displacement components v_s and β take the following form;

$$v_s = R\sum_{i=1}^{N} C_i\phi_{vi}(\theta) = R\{C\}^T\{\phi_v\} \tag{43a}$$

$$\beta = \sum_{i=1}^{N} D_i\phi_{\beta i}(\theta) = \{D\}^T\{\phi_\beta\} \tag{43b}$$

where C_i, D_i = undetermined parameters and $\phi_{vi}(\theta)$, $\phi_{\beta i}(\theta)$ = displacement functions which satisfy the boundary conditions. Since the arch is supported at its both ends, the boundary conditions are, from eqns (A2) in Appendix 1;

$$v_s = 0, \quad \beta = 0, \quad v_s' = 0 \quad \text{and} \quad \beta' - v_s'/R = 0 \quad \text{at} \quad \theta = \pm\theta_0 \tag{44}$$

where θ_0 is the half subtended angle of the arch (Fig. 3). Using eqns (20), eqns (44) reduce to

$$v_s = v_s' = \beta = \beta' = 0. \tag{45}$$

Thus, we shall use the following deflection function to satisfy the above boundary conditions:

$$\phi_{vi}(\theta) = \phi_{\beta i}(\theta) = \cos i\pi\frac{\theta}{\theta_0} - \cos i\pi. \tag{46}$$

The in-plane forces $\bar{q}_x^{(0)}$ and $\bar{q}_\theta^{(0)}$ are, respectively, the x and θ components of the load q per unit arc length of the arch (Fig. 3). Thus,

$$\bar{q}_x^{(0)} = -q\cos^2\theta \tag{47a}$$

$$\bar{q}_\theta^{(0)} = q\cos\theta\sin\theta. \tag{47b}$$

The x coordinate of the point of application of the load, x_p, is

$$x_p = \{(h_c + R) - R\cos\theta\}\cos\theta. \tag{48}$$

Substituting eqns (42), (43), (46)–(48) into the virtual work equation (39) leads to the

following homogeneous equation:

$$([K_1]+\lambda[K_2]+\lambda[K_3]+\lambda[K_4])\begin{Bmatrix}\{C\}\\ \{D\}\end{Bmatrix}=0 \tag{49}$$

where $[K_1]$ = stiffness matrix, $[K_2]$ = geometric matrix (i.e. matrix containing initial in-plane stresses), $[K_3]$ = matrix containing initial in-plane displacements and $[K_4]$ = matrix containing initial in-plane external forces. The quantity λ is a non-dimensional load parameter defined as

$$\lambda=\frac{qRL^2}{EI_x} \tag{50}$$

where L is the arc length of the circular arch. The matrices $[K_1]$ to $[K_4]$ are given in Appendix 3, where the following non-dimensional parameters are used:

$$\psi=\frac{EI_\omega}{R^2EI_x},\quad \mu=\frac{EI_{\omega xy}}{R^2EI_x},\quad \kappa=\frac{EI_x}{R^2EA},$$
$$\gamma=\frac{GK_T}{EI_x},\quad \alpha=\frac{EI_x}{EI_y}. \tag{51}$$

The cross-sectional properties A, I_x, I_y, I_ω and K_T are obtained from eqns (30) with $R_s = r$, and $I_{\omega xy}$ is defined by

$$I_{\omega xy}=\int_A \omega xy\,dA. \tag{52}$$

It is to be noted that the value of $I_{\omega xy}$ is equal to $-I_\omega$ for double symmetric I-section which is used in this numerical example.

Thus, the buckling load λ is computed from the condition that the determinant of the coefficient matrix in eqn (49) is zero.

3.4 *Numerical results*

In this numerical example, the first four terms of the displacement function given in eqn (46) are used in the computation.

First of all, the computer buckling loads are compared with Namita's results for the Case I $|[K_1]+\lambda[K_2]|=0$ where the initial in-plane displacements are neglected and the uniformly distributed load is applied at the centre of gravity of the cross section of the arch. For the purpose of comparison, these computed buckling loads are plotted on Namita's curves as shown in Figs. 4 and 5 for rise-span ratio, (a/b), equal to 0.1 and 0.2 respectively. It can be seen that the computed buckling loads are more or less the same with Namita's results for (a/b) equal to 0.1 in Fig. 4; and in Fig. 5 for (a/b) equal to 0.2, they are also more or less the same when the γ is within the range of 10^{-4} to 10^{-2} but they are smaller when the γ is in the range of

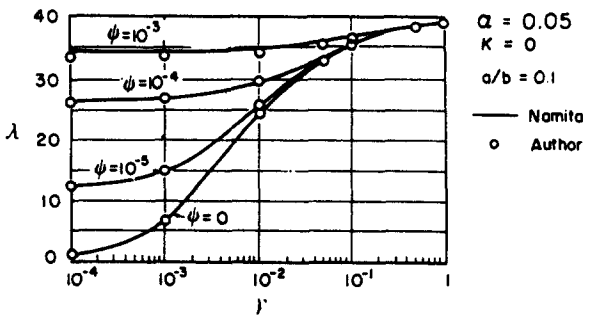

Fig. 4. Comparison of the computed and Namita's[12] results $(a/b = 0.1)$.

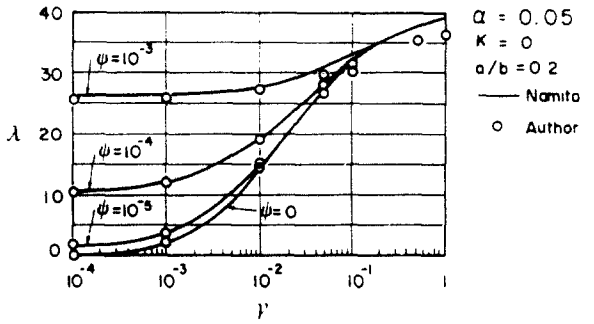

Fig. 5. Comparison of the computed and Namita's[12] results ($a/b = 0.2$).

10^{-2} to 1. This is a result to be anticipated since, as discussed in Appendix 1, the presently derived equations of equilibrium for out-of-plane deformations are somewhat different from those derived by Namita.

The effects of initial pre-buckling displacements on the buckling loads are shown in Table 1. In the columns indicating I the buckling loads for Case I $|[K_1] + \lambda[K_2]| = 0$ are listed, and in the II columns the buckling loads for Case II $|[K_1] + \lambda[K_2] + \lambda[K_3]| = 0$, where the initial in-plane displacements are considered, are listed. The values with bracket are the percentage increases in the buckling loads due to the initial in-plane displacements. The values of ψ and κ are fixed, while the values of the parameters a/b, α and γ are varied. It is seen that the effects of the initial displacements are significant only for very shallow arches with the smaller value of γ (i.e. torsionally weak shallow arches). When the rise-span ratio a/b exceeds 0.05, the pre-buckling displacements have almost negligible effects on the buckling loads regardless of the values of α and γ. It is also seen that in such arches the buckling loads are not much affected by α.

The effect of parameter $\kappa = (EI_x/R^2EA)$ on the buckling loads are shown in Figs. 6 and 7 for the rise-span ratio (a/b) equal to 0.1 and 0.2, respectively. It is clear that the value of κ has a significant effect on the buckling loads in the case of (a/b) equal to 0.1 and the buckling loads are larger if the κ values are smalller. In other words, if EI_x is kept constant, the arches with larger radius of curvature and larger cross-sectional area have higher non-dimensional buckling loads. On the other hand, the effect of the values of κ on the buckling loads is not significant for the case of (a/b) equal to 0.2. Furthermore, it can be seen from Figs. 6 and 7 that the arches with higher warping torsional rigidity have larger buckling loads; and the effect of warping torsional rigidity is significant for arches with small St. Venant torsional rigidity. Therefore, if the warping torsional rigidity is neglected in the analysis, then the buckling loads would be

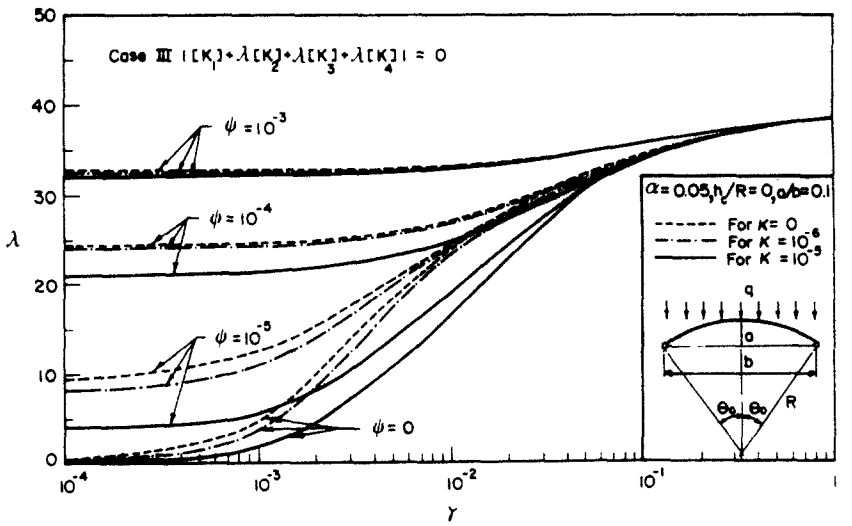

Fig. 6. Effect of parameter κ ($a/b = 0.1$).

Table 1. The effects of initial in-plane displacements on the buckling loads

$\psi = 10^{-3}$, $\kappa = 10^{-4}$

	a/b = 0.025				a/b = 0.05				a/b = 0.1				a/b = 0.2			
	γ = 1.0		γ = 0.01		γ = 1.0		γ = 0.01		γ = 1.0		γ = 0.01		γ = 1.0		γ = 0.01	
α	I	II	I	II	I	II	I	II	I	II	I	II	I	II	I	II
0.1	180.12	191.41	69.265	74.162	54.598	55.023	28.074	28.660	39.290	39.341	23.402	23.478	35.960	36.020	10.346	10.343
	(6.27)		(7.07)		(0.778)		(1.73)		(0.130)		(0.329)		(0.167)		(-0.029)	
0.25	128.18	137.60	66.927	77.608	45.808	46.078	32.324	33.475	38.822	38.879	24.871	24.983	35.963	36.100	10.666	10.652
	(7.35)		(15.9)		(0.589)		(3.56)		(0.144)		(0.450)		(0.381)		(-0.130)	
0.5	91.473	96.274	62.791	78.054	42.586	42.805	33.883	35.282	38.663	38.732	25.366	25.521	35.964	36.227	10.775	10.743
	(5.25)		(24.3)		(0.514)		(4.13)		(0.178)		(0.611)		(0.731)		(-0.297)	
0.75	75.727	78.656	59.205	73.873	41.482	41.685	34.327	35.787	38.610	38.691	25.532	25.725	35.965	36.352	10.812	10.759
	(3.87)		(24.8)		(0.489)		(4.25)		(0.210)		(0.756)		(1.076)		(-0.490)	
1.0	67.196	69.252	56.340	68.344	40.925	41.120	34.521	36.005	38.583	38.677	25.615	25.843	35.965	36.476	10.831	10.754
	(3.06)		(21.3)		(0.476)		(4.30)		(0.244)		(0.902)		(1.421)		(-0.711)	

Note: I and II indicate the cases where the initial in-plane displacements are neglected and considered, respectively, and the values with brackets are the percentage increases in the buckling load λ due to the initial in-plane displacements.

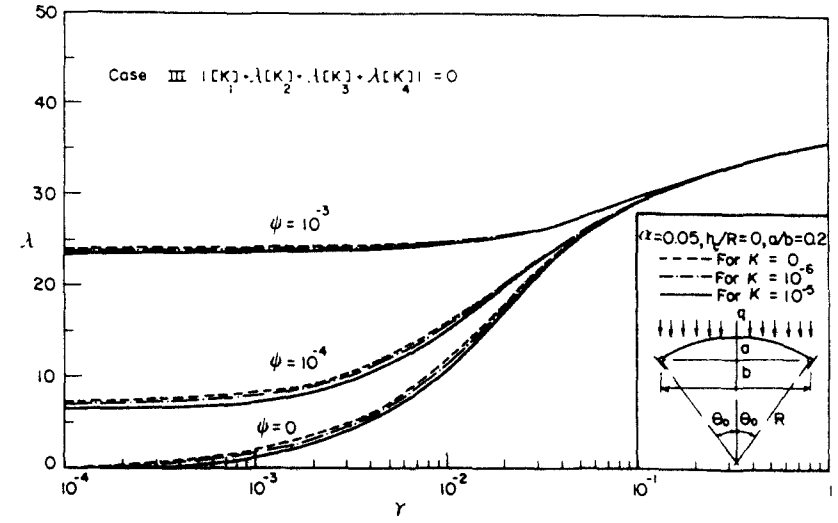

Fig. 7. Effect of parameter κ ($a/b = 0.2$).

underestimated. On the other hand, if the arches have higher St. Venant torsional rigidity the buckling loads become larger and the effect of warping torsional rigidity becomes insignificant. Moreover, it also can be seen that all the curves converge to a point at $\gamma = 1$, i.e. the St. Venant torsional rigidity equal to the lateral flexural rigidity. This converged buckling load is independent of warping torsional rigidity and parameter κ.

The effect of the matrix $[K_4]$ on the buckling load is illustrated in Figs. 8 and 9 for the rise-span ratio a/b equal to 0.1 and 0.2 respectively. The matrix $[K_4]$ reflects the so-called tipping effect[22] that is caused by the in-plane load located above the arch centroidal axis. In Case II the matrix $[K_4]$ is neglected in the calculations, while in Case III it is considered with $h_c = 0.0$ (i.e. the in-plane load is assumed to be applied on the horizontal projection tangent to the arch at the crown). It can be seen that, from these figures, the buckling loads for Case II always higher than the Case III under all values of ψ, γ and κ for (a/b) equal to 0.1 and 0.2 as shown in Figs. 8 and 9. One important point to be mentioned is that the two different loading conditions will not change the converged buckling load of the arches at $\gamma = 1$.

The effects of h_c, that is the distances between the crown and the uniformly distributed load applied on the horizontal projection, on the buckling load are shown in Figs. 10 and 11 for (a/b) equal to 0.1 and 0.2, respectively. The values of κ equal to 10^{-6} and ψ equal to 10^{-3} are used in

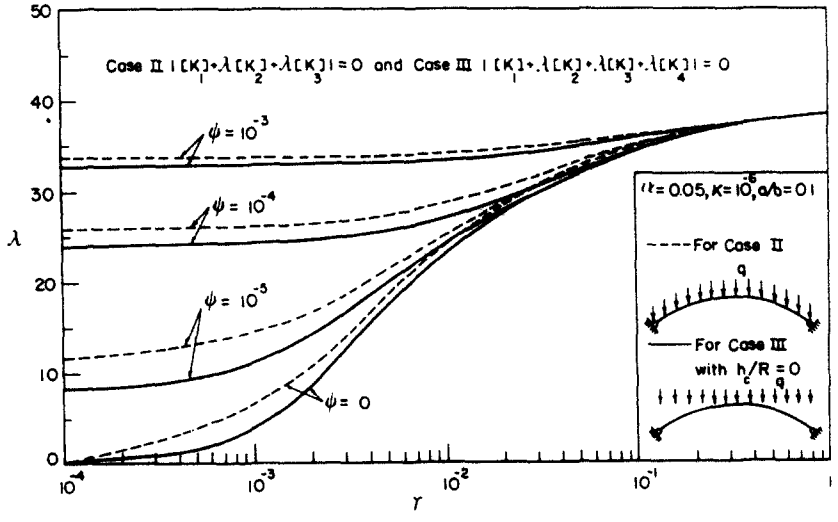

Fig. 8. Effect of loading conditions ($a/b = 0.1$).

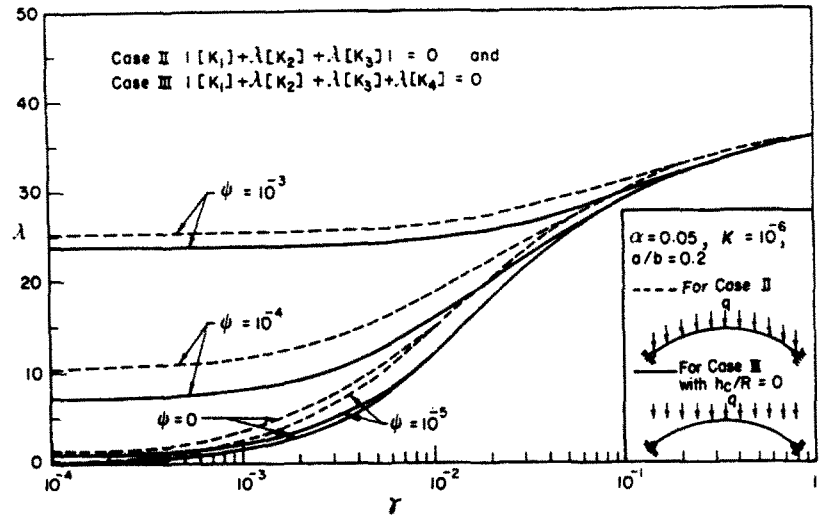

Fig. 9. Effect of loading conditions ($a/b = 0.2$).

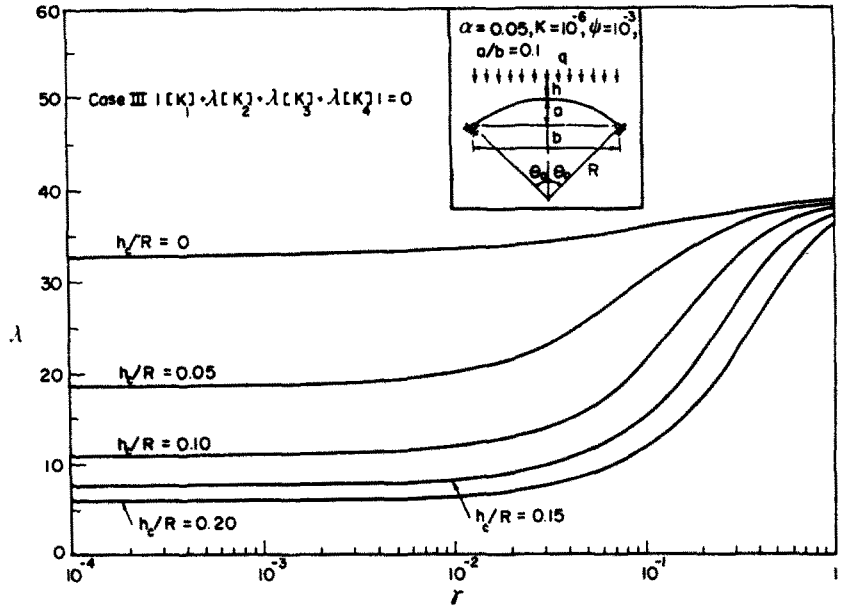

Fig. 10. Effect of h_c/R ratio ($a/b = 0.1$).

this evaluation. It is clear that, the buckling loads are smaller if the loading is far away from the crown of the arch.

4. CONCLUSIONS

In this study, the most important equations are the well established strain-displacement relations (21) for curved members with thin-walled open sections. By using these strain-displacement relations in the variational principles in elasticity, the governing differential equations for equilibrium and the associated boundary conditions can be obtained with no difficulty. The advantage of this approach is that the geometric consideration of the deformed member need not be considered in the formulations.

The application of these derived strain-displacement relations is illustrated in the lateral-torsional buckling analysis of circular arches. The governing equation for lateral-torsional buckling is derived by using these relations through the Euler method in variational principles in elasticity. The buckling loads are evaluated under different values of the non-dimensional

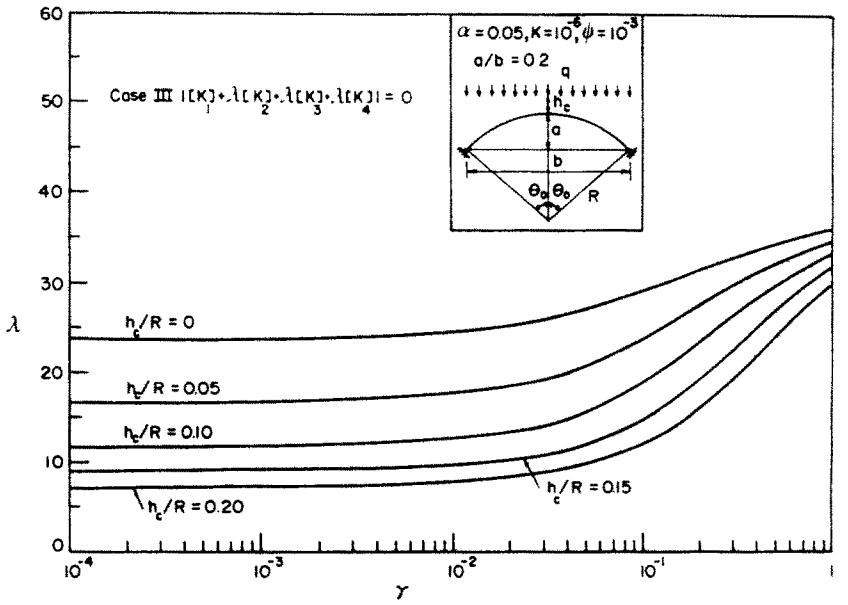

Fig. 11. Effect of h_c/R ratio ($a/b = 0.2$).

parameters

$$\psi = \frac{EI_\omega}{R^2EI_x}, \quad \mu = \frac{EI_{\omega xy}}{R^2EI_x}, \quad \kappa = \frac{EI_x}{R^2EA},$$

$$\gamma = \frac{GK_T}{EI_x}, \quad \alpha = \frac{EI_x}{EI_y}, \quad \frac{a}{b} \text{ and } \frac{h_c}{R}.$$

REFERENCES

1. V. Z. Vlasov, *Thin Walled Elastic Beams*, OTS61-11400. National Science Foundation, Washington, D.C. (1961).
2. I. Konishi and S. Komatsu, On fundamental theory of thin-walled curved girder. *Trans. Japan Soc. Civ. Engrs* **87**, 35–48 (1962).
3. I. Konishi and S. Komatsu, Three dimensional analysis of curved girders with thin-walled cross section. *IABSE* **25**, 143–204 (1965).
4. J. A. Cheney, Bending and buckling of thin-walled open section rings. *Proc. Am. Soc. Civ. Engrs* **98**, EM5, 17–44 (1963).
5. S. Kuranishi, Analysis of thin-walled curved beam. *Trans. Japan Soc. Civ. Engrs* **108**, 7–12 (1964).
6. Y. Fukasawa, Fundamental theory on static analysis of thin-walled curved bars. *Trans. Japan Soc. Civ. Engrs* **110**, 30–51 (1964).
7. R. Dobrowski, Zur Berechnung von gekrümmten dünnwandigen Trägern mit offenen Profil. *Der Stahlbau* **12**, 364–372 (1964).
8. R. Dabrowski, Wölbkrafttorsion von gekrümmten Kastenträgern mit nichtverformbaren Profil. *Der Stahlbau* **5**, 135–141 (1965).
9. R. N. Nitzsche and R. E. Miller, Torsion and flexure of curved thin-walled beams or tubes. *Proc. Am. Soc. Civ. Engrs* **98**, EM5, 867–889 (1972).
10. H. E. Williams, Linear theory of thin rings. *Proc. Am. Soc. Civ. Engrs* **98**, EM5, 1031–1051 (1972).
11. F. Nishino and Y. Fukasawa, Formulation of static behavior of thin-walled curved beams under assumptions of strain field. *Proc. Japan Soc. Civ. Engrs* **247**, 9–19 (1976).
12. Y. Namita, Die Theorie II. Ordnung von krummen Stäben und ihre Anwendung auf das Kipp-Problem des Bogenträgers. *Trans. Japan Soc. Civ. Engrs* **155**, 32–41 (1968).
13. Y. Enda, Analysis of thin-walled curved beam by the transfer matrix method, in *Advances in Computational Methods in Structural Mechanics and Design* (Edited by R. W. Clough *et al.*), pp. 757–774. The University of Alabama in Huntsville Press, Alabama (1972).
14. Y. Enda, Second-order elastic stress analysis of thin-walled curved beams with open cross section by transfer matrix method. *Proc. Japan Soc. Civ. Engrs* **210**, 1–11 (1973).
15. K. Washizu, *Variational Methods in Elasticity and Plasticity*, 2nd Edn. Pergamon Press, Oxford (1974).
16. S. Usuki, Lateral-torsional buckling of thin-walled circular arch accounting for prebuckling deflections. *Proc. Japan Soc. Civ. Engrs* **263**, 35–48 (1977).
17. V. V. Novozhilov, *Foundations of the Nonlinear Theory of Elasticity*. Graylock Press, New York (1953).
18. S. Nair and G. Hegemier, Effect of initial stresses on the small deformations of a composite rod, *AIAA J.* **16**, 212–217 (1978).
19. F. Nishino, C. Kasemset and S. L. Lee, Variational formulation of stability problems for thin-walled members. *Ingenier-Archiev* **43**, 58–68 (1973).

20. F. Nishino, Y. Kurakata, A. Hasegawa and T. Okumura, Thin-walled members under axial force, bending and torsion. *Proc. Japan Soc. Civ. Engrs* **247**, 9–19 (1976).
21. T. V. Galambos, *Structural Members and Frames*. Prentice Hall, Englewood Cliffs, New Jersey (1968).
22. B. G. Johnson (Editor), *The Guide to Stability Design Criteria for Metal Structures*, 3rd Edn. Wiley, New York (1976).
23. K. Klöppel and W. Protte, Ein Beitrag zum Kipp-Problem des kreisförmig gekrümmten Stabes. *Der Stahlbau* **30**, 1–15 (1961).
24. S. Kuranishi, Torsional buckling strength of solid rib arch bridge. *Trans. Japan Soc. Civ. Engrs* **75**, 59–65 (1961).
25. Y. Fukasawa, The buckling of curcular arches by lateral, flexure and torsion under axial thrust. *Proc. Japan Soc. Civ. Engrs* **96**, 29–47 (1963).
26. P. Vachrajittiphan and N. S. Trahair, Flexural-torsional buckling of curved members. *Proc. Am. Soc. Civ. Engrs* **101**, ST6, 1223–1238 (1975).

APPENDIX 1

The derived governing differential equations for equilibrium and the associated boundary conditions are given herein. For simplicity only those equations that are derived expanding $\sin\beta$ and $\cos\beta$ in eqns (21) in Taylor series and neglecting the terms higher than $O(\epsilon^2)$ are shown.

Equations of equilibrium

$$\text{(a)}\quad \frac{N'}{R_s}+\frac{Q_x}{R_s}+\bar{q}_\theta=0 \tag{A1a}$$

$$\text{(b)}\quad \frac{Q_x'}{R_s}-\frac{N}{R_s}-\frac{1}{R_s^2}\{\tilde{N}u_s-(\tilde{M}_x-y_s\tilde{N})\beta\}+\bar{q}_x=0 \tag{A1b}$$

$$\text{(c)}\quad \frac{Q_y'}{R_s}+\bar{q}_y=0 \tag{A1c}$$

$$\begin{aligned}\text{(d)}\quad &\frac{T'}{R_s}+\frac{1}{R_s}\{M_x-y_sN+(M_y-x_sN)\beta\}+\frac{1}{R_s^2}\Big[-\Big(M_x-\frac{M_\omega}{R_s}\Big)(u_s''-w_s')\\&+M_yv_s''+N'\{x_sv_s'-y_s(u_s'-w_s)\}+(\tilde{M}_x-y_s\tilde{N})u_s\\&-M_{sv}(u_s'-w_s)-K_y\beta\Big]+\bar{m}_\theta+\frac{1}{R_s}\Big\{\Big(\bar{m}_x-\frac{\bar{m}_\omega}{R_s}\Big)(u_s'-w_s)-\bar{m}_yv_s'-R_s\bar{m}_{xv}\beta\Big\}=0\end{aligned} \tag{A1d}$$

where

$$\begin{aligned}Q_x=&\frac{1}{R_s}\Big[M_y'-x_sN'+A_1(u_s'-w_s)-A_3\Big(\beta'-\frac{v_s'}{R_s}\Big)-\Big(M_x'-y_sN'-M_{sv}-\frac{M_\omega'}{R_s}\Big)\beta\Big]\\&+\bar{m}_y-\Big(\bar{m}_x-\frac{\bar{m}_\omega}{R_s}\Big)\beta\end{aligned} \tag{A2a}$$

$$\begin{aligned}Q_y=&\frac{1}{R_s}\Big[M_x'-y_sN'-M_{SV}-\frac{M_\omega'}{R_s}+\tilde{N}v_s'+\{(\tilde{M}_y-x_s\tilde{N})\beta\}'+\frac{1}{R_s}\Big\{A_3(u_s'-w_s)\\&-A_2\Big(\beta'-\frac{v_s'}{R_s}\Big)\Big\}\Big]+\bar{m}_x-\frac{\bar{m}_\omega}{R_s}+\bar{m}_y\beta\end{aligned} \tag{A2b}$$

$$\begin{aligned}T=M_{SV}+&\frac{1}{R_s}\Big[M_\omega'+\Big(M_x-\frac{M_\omega}{R_s}-A_3\Big)(u_s'-w_s)+(\tilde{M}_y-M_y-x_s\tilde{N})v_s'\\&+A_2\Big(\beta'-\frac{v_s'}{R_s}\Big)+K_x\beta'\Big]+\bar{m}_\omega\end{aligned} \tag{A2c}$$

$$A_1=\tilde{N}+2\frac{\tilde{M}_y-x_s\tilde{N}}{R_s}+\frac{K_x}{R_s^2} \tag{A2d}$$

$$A_2=K_y-2\frac{K_{\omega x}}{R_s}+\frac{K_\omega}{R_s^2} \tag{A2e}$$

$$A_3=\tilde{M}_x-y_s\tilde{N}-\frac{\tilde{M}_\omega}{R_s}+\frac{K_{xy}}{R_s}-\frac{K_{\omega x}}{R_s^2} \tag{A2f}$$

Boundary conditions

$$\text{(a)}\quad w_s+\frac{x_s}{R_s}(u_s'-w_s)+\frac{y_s}{R_s}v_s'=\bar{C}_1\quad\text{or}\quad N=\nu_\theta\tilde{N} \tag{A3a}$$

$$\text{(b)}\quad u_s=\bar{C}_2\quad\text{or}\quad Q_x=\nu_\theta\tilde{Q}_x \tag{A3b}$$

$$\text{(c)}\quad u_s'-w_s=\bar{C}_3\quad\text{or}\quad M_y-\Big(M_x-\frac{M_\omega}{R_s}\Big)\beta=\nu_\theta\Big\{\tilde{M}_y-\Big(\tilde{M}_x-\frac{\tilde{M}_\omega}{R_s}\Big)\beta\Big\} \tag{A3c}$$

$$\text{(d)}\quad v_s=\bar{C}_4\quad\text{or}\quad Q_y=\nu_\theta\tilde{Q}_y \tag{A3d}$$

$$\text{(e)}\quad v_s'=\bar{C}_5\quad\text{or}\quad M_x+M_y\beta=\nu_\theta(\tilde{M}_x+\tilde{M}_y\beta) \tag{A3e}$$

$$\text{(f)}\quad \beta = \bar{C}_6 \quad \text{or} \quad T = \nu_\theta \left\{ \bar{T} + \frac{\bar{M}'_\omega}{R_s} + \frac{1}{R_s}\left(\bar{M}_x - \frac{\bar{M}_\omega}{R_s}\right)(u'_s - w_s) - \frac{\bar{M}_y}{R_s} v'_s - \bar{T}_{xy}\beta \right\} \tag{A3f}$$

$$\text{(g)}\quad \beta' - \frac{v'_s}{R_s} = \bar{C}_7 \quad \text{or} \quad M_\omega = \nu_\theta \bar{M}_\omega \tag{A3g}$$

where $\bar{C}_1 \sim \bar{C}_7$ are prescribed values at the boundaries.

Now the derived equations of equilibrium are compared with those obtained elsewhere[12–14, 18]. In the present derivations the axial displacement w_s has been defined at the same reference point as u_s and v_s (i.e. point S) while in the other studies the axial displacement is defined at the origin of the coordinates (i.e. point 0). This makes the direct comparisons difficult and therefore it is assumed that the cross section is such that $x_s = y_s = 0$. When the initial radius of curvature of the member is large as compared with its crosssectional dimensions (i.e. $r = R_s$), the following approximations are valid (see eqns 28):

$$\bar{N} = N, \quad \bar{M}_x = M_x, \quad \bar{M}_y = M_y, \quad \bar{M}_\omega = M_\omega. \tag{A4}$$

If eqns (A4) and $x_s = y_s = 0$ are substituted into eqns (A1) and (A2), and the underlined terms in those equations are neglected, the resulting equations become exactly the same as those derived by Enda[13, 14]. The differences of the Enda's equations from the present ones result from the following additional approximations made by him: (1) The nonlinear term u^2 in eqn (3b) has been neglected; (2) The linearized expression for the rate of twist (i.e. the term following ω in eqn 19) has been used; and (3) The distributed external moments $\bar{m}_x$, $\bar{m}_y$, $\bar{m}_\omega$ and $\bar{m}_{xy}$ have not been considered.

Next the present equations of equilibrium are compared with those derived by Namita[12]. It has been found that Namita's equations are somewhat different from those obtained by the authors as well as Enda. For comparison Namita's equations corresponding to eqns (A1c) and (A1d) (out-of-plane equilibrium equations) are shown below:

$$\frac{1}{R_s^2}\left[\left\{M'_x - M_{SV} - \frac{M'_\omega}{R_s}\right\}' + N(v''_s + R_s\beta) + \left\{M_y\left(\beta' - \frac{v'_s}{R_s}\right)\right\}' + M'_y\left(\beta' - \frac{v'_s}{R_s}\right)\right] + \frac{1}{R_s}\left\{\bar{m}'_x + \bar{m}_y\left(\beta' - \frac{v'_s}{R_s}\right)\right\} + \bar{q}_y = 0 \tag{A5a}$$

$$\frac{M'_{sv}}{R_s} + \frac{1}{R_s}(M_x - M_y\beta) + \frac{1}{R_s^2}[M''_\omega + \{(K_x + K_y)\beta'\}' - M_x(u''_s - w'_s) - M_y(v''_s + R_s\beta)] + \bar{m}_\theta = 0. \tag{A5b}$$

It is seen that the expressions for the underlined terms in eqn (A5a) are different from the corresponding terms in eqn (A1c) with eqn (A2b). It is to be noted that in the case of a straight member the equilibrium equations derived by the authors and by Enda reduce to the presently accepted equations [19]–[21], while the Namita's equation (A5a) fails to agree with the equation.

Last comparison is made with the equations of equilibrium derived by Nair and Hegemier[18]. The equations for out-of-plane deformations can be written, using the present notation, as follows:

$$\frac{Q'_y}{R_s} + \bar{q}_y = 0 \tag{A6a}$$

$$\frac{M'_{SV}}{R_s} + \frac{M_x}{R_s} + \frac{1}{R_s^2}\left[\left\{(K_x + K_y)\left(\beta' - \frac{v''_s}{R_s}\right)\right\}' - M_x(u''_s - w'_s) + M_y v''_s + M_x(u_s + w'_s) - M_{SV}(u'_s - w_s) - K_y\left(\beta + \frac{v''_s}{R_s}\right) - \frac{K_{xy}}{R_s}(u''_s - w'_s)\right] + \bar{m}_\theta + \frac{1}{R}\{\bar{m}_x(u'_s - w_s) - \bar{m}_y v'_s\} = 0 \tag{A6b}$$

where

$$Q_y = \frac{1}{R_s}\left[M'_x - M_{sv} + Nv'_s + (M_y\beta)' - 2M_y\frac{v'_s}{R_s} + \frac{1}{R_s}\left\{M_x(u'_s - w_s + (u_s + w'_s)') - (K_x + K_y)\left(\beta' - \frac{v'_s}{R_s}\right) + M_{SV}(u_s + w'_s) - \left(K_y\left(\beta + \frac{v''_s}{R_s}\right)\right)' - \left(\frac{K_{xy}}{R_s}(u'_s - w_s)\right)'\right\}\right] + \bar{m}_x\left\{1 - \frac{1}{R_s}(u_s + w'_s)\right\} + \bar{m}_y\beta. \tag{A6c}$$

It is to be noted that the original equations contain some additional terms (denoted by $P^{(0)}_{\alpha\beta}$ in Ref.[18]) concerning with the transverse shearing stresses. Note that Hair and Hegemier have not considered the warping torsional effects. Eqautions (A6) are quite similar in form to eqns (A1c, d) with (A2b, c) if the conditions of eqns (A4), $x_s = y_s = 0$ and $M_\omega = \bar{M}_\omega = \bar{m}_\omega = 0$ are introduced; however slight differences are found in the underlined terms in eqns (A6).

Lastly, mention is made of the fact that when the linearized force-displacement equations shown in Appendix 2 are substituted into the linear terms in eqns (A1) and (A2) we obtain the equations of equilibrium, in terms of the displacement components, that have the same degree of accuracy as the beam-column equations for straight members[21].

APPENDIX 2

Force-displacement relations for small displacement theory of curved members

The linear parts of the force-displacement relations derived with the conditions of eqns (31) are shown below:

$$N = \frac{EA}{R_0}\left[w_s' + u_s + y_s\left(\frac{v_s''}{R_s} + \beta\right) + \frac{x_s}{R_s}(u_s'' - w_s')\right] \tag{A7a}$$

$$M_x = -\frac{1}{R_0}\left[EI_x\left(\frac{v_s''}{R_s} + \beta\right) + \frac{EI_{xy}}{R_s}(u_s'' - w_s')\right] \tag{A7b}$$

$$M_y = -\frac{1}{R_0}\left[EI_{xy}\left(\frac{v_s''}{R_s} + \beta\right) + \frac{EI_x}{R_s}(u_s'' - w_s')\right] \tag{A7c}$$

$$M\omega = \frac{EI_\omega}{R_s^2}\left(\frac{v_s''}{R_s} + \beta''\right) \tag{A7d}$$

$$M_{SV} = \frac{GK_T}{R_s}\left(\beta' - \frac{v_s}{R_s}\right). \tag{A7e}$$

APPENDIX 3

The matrices $[K_1]$, $[K_2]$, $[K_3]$ and $[K_4]$ in eqns (49) are given in the following:

$$[K_1] = \int_{-\theta_0}^{\theta_0}\begin{bmatrix}[K_1]_{11} & [K_1]_{12}\\ [K_1]_{12}^T & [K_1]_{22}\end{bmatrix}\mathrm{d}\theta \tag{A8a}$$

$$[K_2] = \int_{-\theta_0}^{\theta_0}\begin{bmatrix}[K_2]_{11} & [K_2]_{12}\\ [K_2]_{12}^T & [K_2]_{22}\end{bmatrix}\frac{1}{4\theta_0^2}\mathrm{d}\theta \tag{A8b}$$

$$[K_3] = \int_{-\theta_0}^{\theta_0}\begin{bmatrix}[K_3]_{11} & [K_3]_{12}\\ [K_3]_{12}^T & [K_3]_{22}\end{bmatrix}\frac{\alpha}{4\theta_0^2}\mathrm{d}\theta \tag{A8c}$$

$$[K_4] = \int_{-\theta_0}^{\theta_0}\begin{bmatrix}0 & [K_4]_{12}\\ [K_4]_{12}^T & [K_4]_{22}\end{bmatrix}\frac{1}{4\theta_0^2}\mathrm{d}\theta \tag{A8d}$$

where

$$[K_1]_{11} = (1+\psi)\{\phi_v''\}\{\phi_v''\}^T + \gamma\{\phi_v'\}\{\phi_v'\}^T$$

$$[K_1]_{12} = \{\phi_v''\}\{\phi_\beta\}^T - \psi\{\phi_v''\}\{\phi_\beta''\}^T - \gamma\{\phi_v'\}\{\phi_\beta'\}^T$$

$$[K_1]_{22} = \{\phi_\beta\}\{\phi_\beta\}^T + \psi\{\phi_\beta''\}\{\phi_\beta''\}^T + \gamma\{\phi_\beta'\}\{\phi_\beta'\}^T$$

$$[K_2]_{11} = \left(\frac{N^{(0)}}{qR}(1+\kappa+\kappa\psi) - 2\frac{M_y^{(0)}}{qR^2}\mu\alpha\right)\{\phi_v'\}\{\phi_v'\}^T$$

$$[K_2]_{12} = -\left(\frac{N^{(0)}}{qR}\kappa(1+\psi) - 2\frac{M_y^{(0)}}{qR^2}\mu\alpha\right)\{\phi_v'\}\{\phi_\beta'\}^T - \frac{M_y^{(0)}}{qR^2}\{\phi_v''\}\{\phi_\beta\}^T$$

$$[K_2]_{22} = \left(\frac{N^{(0)}}{qR}\kappa\left(1+\frac{1}{\alpha}+\psi\right) - 2\frac{M_y^{(0)}}{qR^2}\mu\alpha\right)\{\phi_\beta'\}\{\phi_\beta'\}^T + \left(\frac{N^{(0)}}{qR}\kappa - \frac{M_y^{(0)}}{qR^2}\right)\{\phi_\beta\}\{\phi_\beta\}^T$$

$$[K_3]_{11} = -(1+\psi)\bar{d}^{(0)}(\{\phi_v'\}\{\phi_v''\}^T + \{\phi_v''\}\{\phi_v'\}^T)$$

$$[K_3]_{12} = -((1+\psi)\bar{d}^{(0)\prime} - \bar{u}_s^{(0)})\{\phi_v''\}\{\phi_\beta\}^T + \bar{d}^{(0)}(\psi\{\phi_v'\}\{\phi_\beta''\}^T - \{\phi_v'\}\{\phi_\beta\}^T)$$

$$[K_3]_{22} = \psi\bar{d}^{(0)\prime}(\{\phi_\beta\}\{\phi_\beta''\}^T + \{\phi_\beta''\}\{\phi_\beta\}^T) - 2(\bar{d}^{(0)\prime} - \bar{u}_s^{(0)})\{\phi_\beta\}\{\phi_\beta\}^T$$

$$[K_4]_{12} = \left(1 + \frac{h_c}{R} - \cos\theta\right)\cos^2\theta\sin\theta\{\phi_v'\}\{\phi_\beta\}^T$$

$$[K_4]_{22} = -\left(1 + \frac{h_c}{R} - \cos\theta\right)\cos^3\theta\{\phi_\beta\}\{\phi_\beta\}^T$$

$$\bar{d}^{(0)} = \frac{EI_y}{qR^4}(u_s^{(0)\prime} - w_s^{(0)})$$

$$\bar{u}_s^{(0)} = \frac{EI_y}{qR^4}u_s^{(0)} \tag{A9a–m}$$